ANALYTICAL SCIENCES OCTOBER 2014, VOL. 30

Investigation of Inner and Outer Phase Formation in Tube Radial Distribution Phenomenon Using Various Types of Mixed Solvent Solutions

Satoshi FUJINAGA,* Katsuya UNESAKI,* Yuki KAWAI,* Koichi KITAGUCHI,* Kosuke NAGATANI,* Masahiko HASHIMOTO,* Kazuhiko TSUKAGOSHI,*,*† and Jiro MIZUSHIMA****

**Department of Chemical Engineering and Materials Science, Faculty of Science and Engineering, Doshisha University, Kyotanabe, Kyoto 610-0321, Japan*
***Department of Mechanical and Systems Engineering, Faculty of Science and Engineering, Doshisha University, Kyotanabe, Kyoto 610-0321, Japan*
****Tube Radial Distribution Phenomenon Research Center, Doshisha University, Kyotanabe, Kyoto 610-0321, Japan*

When mixed solvent solutions, such as ternary water–hydrophilic/hydrophobic organic solvents, water–surfactant, water–ionic liquid, and fluorous–organic solvents are delivered into a microspace under laminar flow conditions, the solvent molecules are radially distributed in the microspace, generating inner and outer phases. This specific fluidic behavior is termed "tube radial distribution phenomenon" (TRDP). In this study, the factors influencing the formation of inner and outer phases in the TRDP using the above-mentioned mixed solvent solutions were investigated. We examined phase diagrams, viscosities of the two phases (upper and lower phases in a batch vessel), volume ratios of the phases, and bright-light or fluorescence photographs of the TRDP. When the difference in viscosities between the two phases was large (> approximately 0.73 mPa·s), the phase with the larger viscosity formed an inner phase regardless of the volume ratios, whereas when the difference was small (< approximately 0.42 mPa·s), the phase with the larger volume formed an inner phase. The TRDP using a water–surfactant mixed solution was also investigated in capillary chromatography based on TRDP.

Keywords Tube radial distribution phenomenon (TRDP), phase separation, viscosity, tube radial distribution chromatography (TRDC)

(Received May 1, 2014; Accepted September 1, 2014; Published October 10, 2014)

Introduction

The phase separation of aqueous systems containing polymers, micelles, and ionic liquids is well known, and has been used in the fields of analytical chemistry and separation science since the last century.[1-5] For example, aqueous micellar solutions of specific non-ionic surfactants separate into two distinct phases when heated above a certain temperature (cloud point), *i.e.*, a temperature-induced phase separation occurs.[6-10] One phase behaves as an almost surfactant-free aqueous solution (aqueous phase), whereas the other phase is a concentrated surfactant solution (surfactant-rich phase). Hydrophobic compounds dissolved in the aqueous micellar solution are extracted into the surfactant-rich phase, whereas hydrophilic compounds remain in the aqueous phase.

Fluorous or fluorocarbon chemistry, which involves phase separation processes, has been also investigated since the study reported by Horváth and Rábai in 1994.[11] The phase separation of fluorous (fluorocarbon)–organic (hydrocarbon) solvent mixed solutions has been applied in separation science.[12,13] Mixed solutions of fluorous–organic solvents separate into two distinct phases in a batch vessel when cooled below a certain temperature,[14] with the lower phase comprising an almost pure fluorous solvent and the upper phase consisting of an organic solvent. Based on this phase separation system, liquid–liquid and liquid–solid extractions have been reported using a variety of fluorous solvents.[15-17]

A novel phase separation system involving a ternary mixed solvent system has been reported by our group.[18-21] A ternary mixed solvent solution of water–hydrophilic/hydrophobic solvents changes from a homogeneous (single-phase) to a heterogeneous (two-phase) system in a batch vessel according to temperature and/or pressure changes. Furthermore, when the ternary mixed solvent solution is delivered into a microspace, such as a microchannel on a microchip or a capillary tube, under laminar flow conditions, the solvent molecules are radially distributed in the microspace, generating inner and outer phases. This process is termed "tube radial distribution phenomenon" (TRDP). The TRDP creates a kinetic liquid–liquid interface, but not static, in a microspace. We developed new types of open-tubular capillary chromatography, *i.e.*, tube radial distribution chromatography (TRDC)[22] and microreactors[23]

† To whom correspondence should be addressed.
E-mail: ktsukago@mail.doshisha.ac.jp

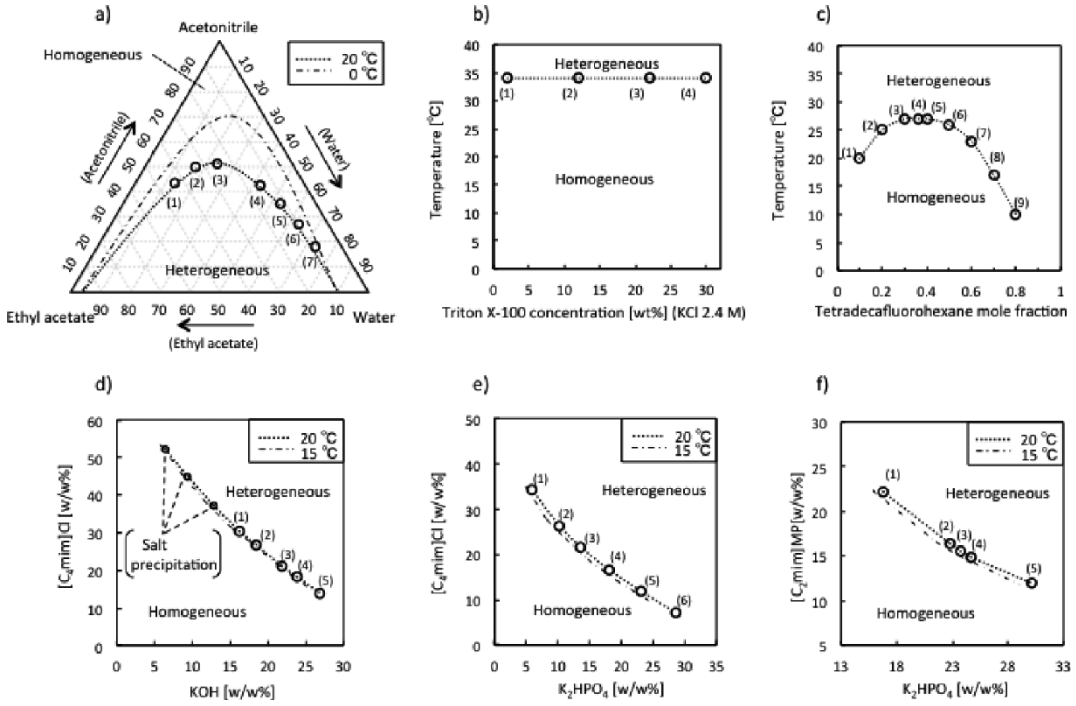

Fig. 1 Phase diagrams incorporating solubility curves of a) water–acetonitrile–ethyl acetate, b) water–Triton X-100–KCl (2.4 M), c) tetradecafluorohexane–hexane, d) water–[C_4mim]Cl–KOH, e) water–[C_4mim]Cl–K_2HPO_4, and f) water–[C_2mim]MP–K_2HPO_4. The homogeneous solution mixtures, at the associated components composition as denoted by the numbers in square brackets in the phase diagrams were used for subsequent experiments.

based on the TRDP. More interestingly, such specific fluidic behavior of TRDP could also be observed in a microspace involving the other two-phase separation solutions such as water–surfactant, water–ionic liquid, and fluorous-organic solvents.[21] All TRDP with various types of mixed solvent solutions were first observed in our laboratory.

In our previous papers,[19,21] we discussed the phase formation of TRDP generated with a ternary mixed solvent solution of water–hydrophilic/hydrophobic solvents from the viewpoints of the volume ratios of the phases. However, comprehensive information about the factors influencing the formation of the inner and outer phases in the TRDP is still lacking for various types of mixed solutions. To this effect, the phase diagrams, viscosities of the two phases (upper and lower phases) in a batch vessel, volume ratios of the phases, and bright-light or fluorescence photograph of the TRDP were examined by using six kinds of phase separation solutions. General discussion on the formation of TRDP has been based on the experimental data, and the TRDP with water–surfactant mixed solution was applied as an attempt to a capillary TRDC, leading to a clue of expanding various TRDP to their applications with distinguished features.

Experimental

Reagents and materials

Water was purified with an Elix 3 UV system (Millipore Co., Billerica, MA). All reagents used were obtained commercially and were of analytical grade. Perylene, Eosin Y, Rhodamine B, Orange G, acetonitrile, ethyl acetate, tetradecafluorohexane, 1-naphthol, and 2,6-naphthalenedisulfonic acid were purchased from Wako Pure Chemical Industries, Ltd. (Osaka, Japan). Triton X-100, Triton X-114, hexane, potassium hydroxide (KOH), potassium chloride (KCl), and dipotassium hydrogenphosphate (K_2HPO_4) were purchased from Nacalai Tesque, Inc. (Kyoto, Japan). Supplies of 1-butyl-3-methylimidazolium chloride ([C_4mim]Cl) and 1-ethyl-3-methylimidazolium methylphosphonate ([C_2mim]MP) were purchased from Tokyo Chemical Industry Co., Ltd. (Tokyo, Japan). Fused-silica capillary tubes (50 or 75 μm i.d.) were purchased from GL Sciences (Tokyo, Japan).

Phase diagrams

Phase diagrams were constructed for the six types of the mixed solvent solutions: ternary water–hydrophilic/hydrophobic organic solvents (water–acetonitrile–ethyl acetate), water–surfactant (water–Triton X-100–KCl), water–ionic liquid (water–[C_4mim]Cl–KOH, water–[C_4mim]Cl–K_2HPO_4, and water–[C_2mim]MP–K_2HPO_4), and fluorous-organic solvents (tetradecafluorohexane–hexane). All phase diagrams, regardless of the composition system, included solubility curves that separated the component ratio areas into homogeneous (single-phase) and heterogeneous (two-phase) areas in a batch vessel.

Viscosity measurement

The homogeneous solutions of all the mixed solvent systems were converted to heterogeneous solution systems that comprised two phases, the upper and lower phases, by changing the temperature. The viscosities of the upper and lower solutions were measured with a viscometer (HAAKE RheoScope 1; Thermo Scientific, Sydney, NSW, Australia).

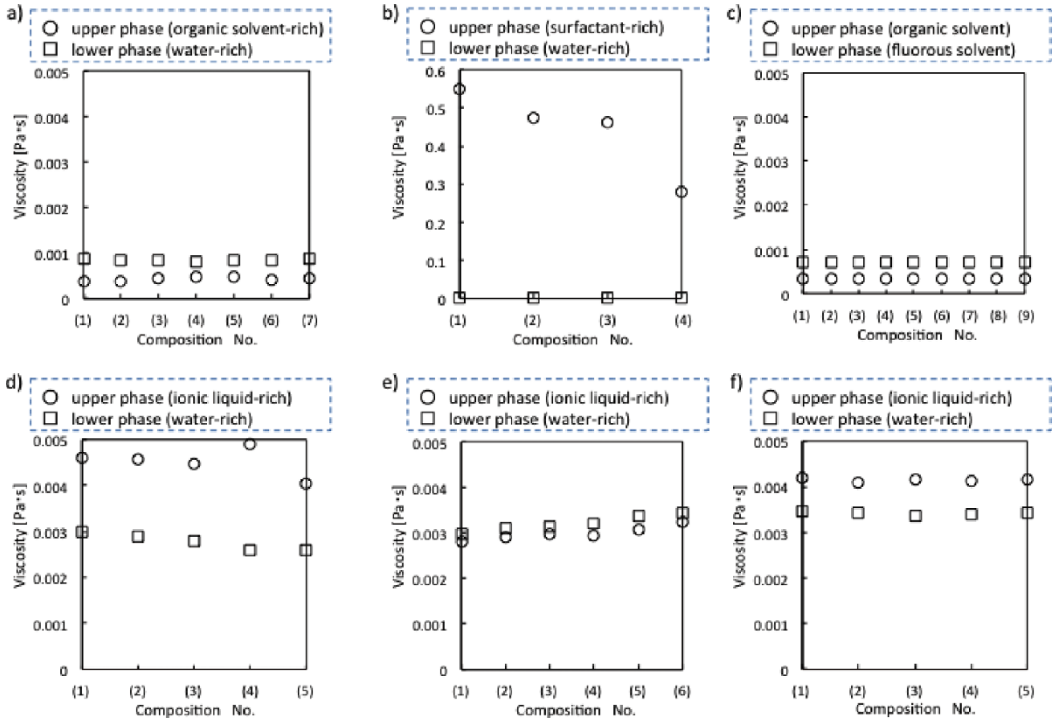

Fig. 2 Viscosities of the (○) upper and (□) lower phases of the solvent mixtures, with different solvent compositions, denoted by the numbers in square brackets in Fig. 1: a) water–acetonitrile–ethyl acetate, b) water–Triton X-100–KCl (2.4 M), c) tetradecafluorohexane–hexane, d) water–[C_4mim]Cl–KOH, e) water–[C_4mim]Cl–K_2HPO_4, and f) water–[C_2mim]MP–K_2HPO_4.

Bright-field or fluorescence microscope–CCD camera system

The bright-field or fluorescence microscope–CCD camera system was equipped with the fused-silica capillary tube. The fluorescent dye-containing mixed solvent solution that was introduced in the capillary tube was observed using a microscope (BX51; Olympus, Tokyo, Japan) and a CCD camera (JK-TU53H; Toshiba, Tokyo, Japan) for bright-field and fluorescence imaging. For the latter imaging, the microscope was equipped with an Hg lamp and a filter (U-MWU2; excitation wavelength: 330 – 385 nm, emission wavelength: > 420 nm). The temperature of the capillary tube was maintained using a thermo-heater (Thermo Plate MATS-555RO; Tokai Hit Co., Shizuoka, Japan).

Capillary TRDC

The open-tubular capillary chromatography, TRDC, mainly comprised a microsyringe pump (MF-9090, Bioanalytical Systems, Inc., West Lafayette, IN), a fused-silica capillary tube (total length: 150 cm and effective length: 100 cm), a thermo-heater, and a fluorescence detector (excitation wavelength: 290 nm and emission wavelength: 355 nm, modified FR-535 fluorescence detector, Shimadzu Co., Kyoto, Japan). An aqueous solution containing 2 wt% Triton X-100 and 2.4 M KCl or 2 wt% Triton X-114 was used as carrier solution. A model analyte solution comprising 1-naphthol (1 mM) and 2,6-naphthalenedisulfonic acid (1 mM) dissolved in the carrier solution was prepared. The analyte solution was injected into the capillary inlet using the gravity method (from 30 cm height and for 30 s), and then fed into the capillary tube at a flow rate of 1.0 μL min^{-1}.

Results and Discussion

Phase diagrams including solubility curves

Phase diagrams were constructed for the six types of mixed solvent systems studied, namely, water–acetonitrile–ethyl acetate, water–Triton X-100–KCl, tetradecafluorohexane–hexane, water–[C_4mim]Cl–KOH, water–[C_4mim]Cl–K_2HPO_4, and water–[C_2mim]MP–K_2HPO_4 (Fig. 1). The compositions shown on the axes of the phase diagrams are different depending on the system studied. The phase diagram of water–acetonitrile–ethyl acetate was based on the solvent volume percentage of each component. The phase diagrams of water–Triton X-100–KCl and tetradecafluorohexane–hexane were constructed according to the relationship between the temperature and concentration of Triton X-100 (wt%) or mole fraction of tetradecafluorohexane. The phase diagram of water–ionic liquid–salt was constructed based on the relationship between the concentrations of the salt and ionic liquid. Regardless, all phase diagrams included solubility curves that separate the component ratio areas of the solvents into the two phases, *i.e.*, homogeneous (single-phase) and heterogeneous (two-phases). In other words, the homogeneous solution changed to a heterogeneous solution or the heterogeneous solution changed to a homogeneous solution upon alteration of the temperature in the batch vessel. The solubility curves in the phase diagrams were constructed by examining the cloud points where the solvent solutions changed from homogeneous (single phase) to heterogeneous (two phases) solutions by adding the solvent (or solute) at a definite temperature or by altering temperature at a definite composition.

The homogeneous mixtures, at the associated component ratios that were positioned near the solubility curves in the phase diagrams and designated by the numbers in square

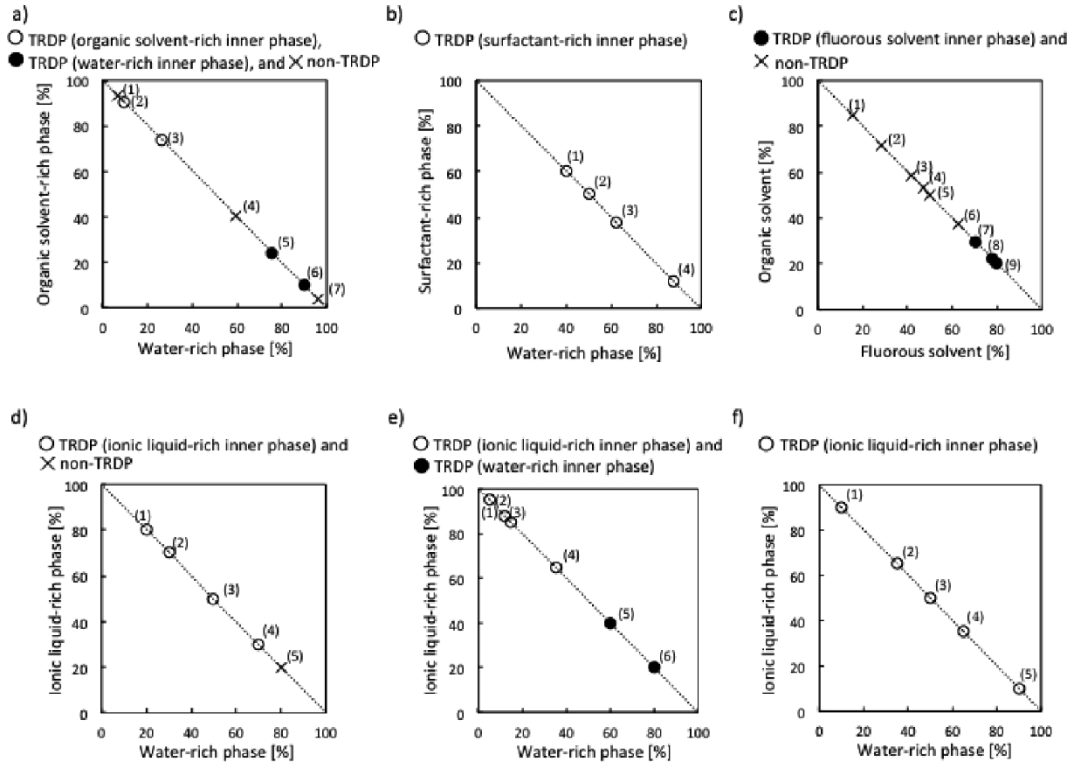

Fig. 3 Relationship between the development of the TRDP and the volume contents of the lower and upper phases. Symbols ○ and ● denote the observation of the TRDP, whereas symbol × implies that the TRDP was not observed. Plots containing symbols ○ and ● show the reversible distribution patterns of the inner and outer phases. The different systems studied were: a) water–acetonitrile–ethyl acetate (flow rate: 0.2 μL min^{-1}; temperature: 0°C); b) water–Triton X-100–KCl (2.4 M) (flow rate: 5.0 μL min^{-1}; temperature: 34°C); c) tetradecafluorohexane–hexane (flow rate: 5.0 μL min^{-1}; temperature: 10°C); d) water–[C_4mim]Cl–KOH (flow rate: 1.0 μL min^{-1}; temperature: 15°C); e) water–[C_4mim]Cl–K_2HPO_4 (flow rate: 1.0 μL min^{-1}; temperature: 15°C); and f) water–[C_2mim]MP–K_2HPO_4 (flow rate: 1.0 μL min^{-1}; temperature: 15°C). Capillary tube inner diameter: a) 50 μm and b) – f) 75 μm.

brackets in the individual phase diagrams (Fig. 1), separated into two phases (upper and lower) in the batch vessel upon change in the temperature. The viscosities and volume ratios of the upper and lower phases were examined; furthermore, the homogeneous solutions were delivered into the capillary tube to observe the TRDP using bright-field or fluorescence microscopy, as discussed in the following sections.

Viscosities of the upper and lower phases

The viscosities of the upper and lower solutions of the different mixed solvent systems following phase separation were examined. The relationship between the designated solution mixture of a specific component's composition and the associated viscosity for each system is shown in Fig. 2. The differences in viscosities between the upper and lower solutions of the water–acetonitrile–ethyl acetate, water–Triton X-100–KCl, tetradecafluorohexane–hexane, water–[C_4mim]Cl–KOH, water–[C_4mim]Cl–K_2HPO_4, and water–[C_2mim]MP–K_2HPO_4 systems were estimated to be respectively 0.42, 440, 0.36, 1.7, 0.22, and 0.73 mPa·s. The system may be tentatively classified according to the degree of difference in viscosities of the upper and lower phases for the following discussion: large (> approximately 0.73 mPa·s) and small (< approximately 0.42 mPa·s). A large viscosity difference between the upper and lower phases was observed for the water–Triton X-100–KCl, water–[C_4mim]Cl–KOH, and water–[C_2mim]MP–K_2HPO_4 systems, whereas a small viscosity difference was observed for the water–acetonitrile–ethyl acetate, tetradecafluorohexane–hexane, and water–[C_4min]Cl–K_2HPO_4 systems.

Volume ratios of the upper and lower phases

The volume ratios of the upper and lower phases of the solvent mixtures designated by the numbers in square brackets in the phase diagrams were evaluated. The upper/lower phase ratios for the mixed solvent systems: water–acetonitrile–ethyl acetate (20 → 0°C), water–Triton X-100-KCl (20 → 34°C), tetradecafluorohexane–hexane (20 → 10°C), water–[C_4mim]Cl–KOH (20 → 15°C), water–[C_4mim]Cl–K_2HPO_4 (20 → 15°C), and water–[C_2mim]MP–K_2HPO_4 (20 → 15°C) varied as a function of the composition ratios which were from 90:10 to 4:96 (organic solvent-rich/water-rich), from 60:40 to 12:88 (surfactant-rich/water-rich), from 85:15 to 20:80 (organic solvent /fluorous solvent), from 80:20 to 20:80 (ionic liquid-rich/water-rich), from 95:5 to 20:80 (ionic liquid-rich/water-rich), and from 90:10 to 10:90 (ionic liquid-rich/water-rich). The volume ratios of the upper and lower phases are shown in Fig. 3.

Evaluation of the TRDP

The homogeneous solutions were delivered to the capillary tube under laminar flow conditions. The solvent behaviors, TRDP and non-TRDP were assessed using bright-field or fluorescence microscopy. Typical photographs showing the

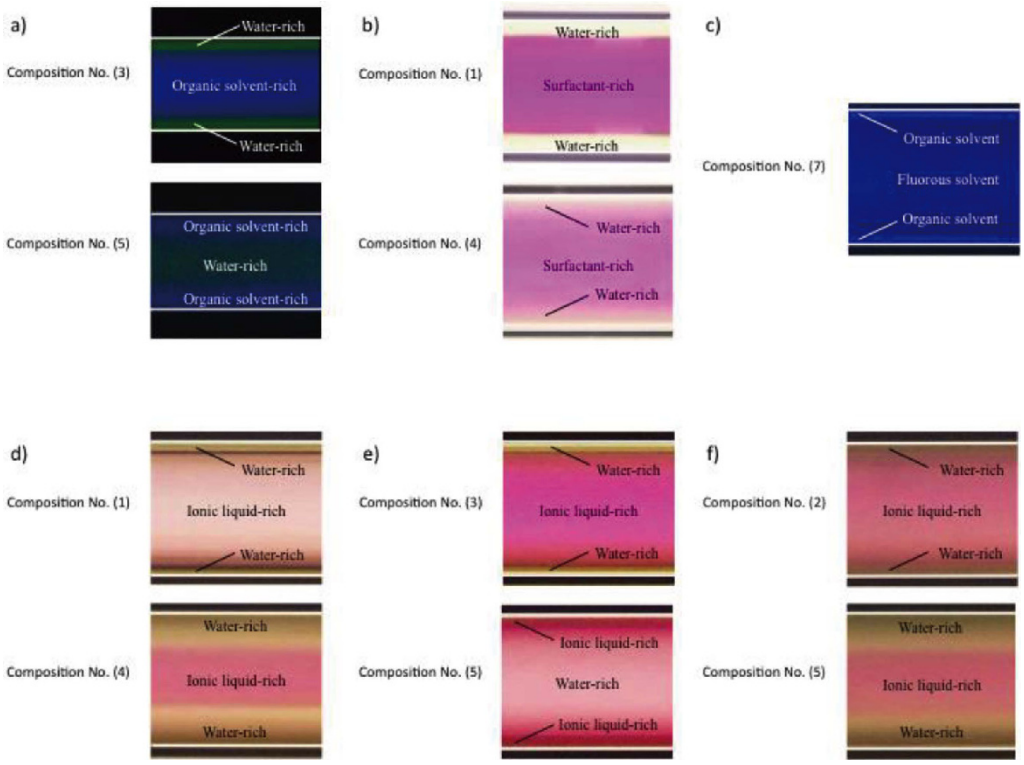

Fig. 4 Bright-field and fluorescence photographs showing the development of the TRDP in the different systems: a) water–acetonitrile–ethyl acetate (flow rate: 0.2 μL min^{-1}; temperature: 0°C; and 1 mM Eosin Y and 0.1 mM perylene); b) water–Triton X-100–KCl (2.4 M) (flow rate: 5.0 μL min^{-1}; temperature: 34°C; and 5 mM Rhodamine B); c) tetradecafluorohexane–hexane (flow rate: 5.0 L min^{-1}; temperature: 10°C; and 0.1 mM perylene); d) water–[C_4mim]Cl–KOH (flow rate: 1.0 μL min^{-1}; temperature: 15°C; and 5 mM Rhodamine B); e) water–[C_4mim]Cl–K_2HPO_4 (flow rate: 1.0 μL min^{-1}; temperature: 15°C; and 2 mM Rhodamine B); and f) water–[C_2mim]MP–K_2HPO_4 (flow rate: 1.0 μL min^{-1}; temperature: 15°C; and 5 mM Rhodamine B). Capillary tube inner diameter: a) 50 μm and b) – f) 75 μm.

development of TRDP are shown in Fig. 4. Interestingly, the solution mixtures of water–Triton X-100–KCl, water–[C_4mim]Cl–KOH, and water–[C_2mim]MP–K_2HPO_4 generated the TRDP in the surfactant-rich inner phase and the ionic liquid-rich inner phase, regardless of the volume ratios of the two phases or component ratios of the solvents. In contrast, the solution mixtures of water–acetonitrile–ethyl acetate, tetradecafluorohexane–hexane, and water–[C_4min]Cl–K_2HPO_4 generated the TRDP in the major volume inner phase and minor volume outer phase. That is, an inverse (reversible) distribution pattern was observed with a change in the volume ratios of the solvents. For example, when considering the water–acetonitrile–ethyl acetate system, introduction of the organic solvent-rich mixed solution to the capillary tube generated an organic solvent-rich major inner phase and a water-rich minor outer phase; in contrast, introduction of the water-rich mixed solution to the capillary tube produced a water-rich major inner phase and an organic solvent-rich minor outer phase.

The TRDP processes in the different mixed solvent systems are denoted by the symbols ○, ●, and ×, and vary according to the lower and upper phases volume content (Fig. 3). The symbols ○ and ● denote the development of TRDP, whereas symbol × implies that TRDP was not observed in a given system at a particular upper/lower volume composition. The mixed solvent systems that include both symbols ○ and ● in the figures demonstrate the occurrence of a reversible distribution pattern of the inner and outer phases in accordance with the phase composition.

Investigation of the inner and outer phase formation

The factors influencing the formation of the inner and outer phases, *i.e.*, non-reversible TRDP or reversible TRDP, were evaluated based on the viscosities and volume ratios of the upper and lower phases, and TRDP observations. When the difference in the viscosities between the two phases was large (> approximately 0.73 mPa·s), the phase with the larger viscosity developed as the inner phase regardless of the volume ratios. Conversely, when the difference in the viscosities between the two phases was small (< approximately 0.42 mPa·s), the phase with the larger volume content formed as the inner phase.

The flow characteristics of two immiscible liquids with different viscosities in a tube were investigated in the last century.[24-27] The experimental studies showed that a low-viscosity fluid had a tendency to encapsulate a high-viscosity fluid. This behavior was in accordance with the viscous-dissipation principle, which postulates that the degree of viscous dissipation is smaller for a given flow rate. Thus, the high-viscosity fluid is located at the core of the tube, away from the inner wall.[24-27] However, in 1984, Joseph *et al.* reported that if the low-viscosity fluid occupies an extremely large volume of space in a tube, the low-viscosity fluid is located at the core of the tube rather than near the wall of the tube, regardless of the viscosity values.[28] The discussions relating to the inner and

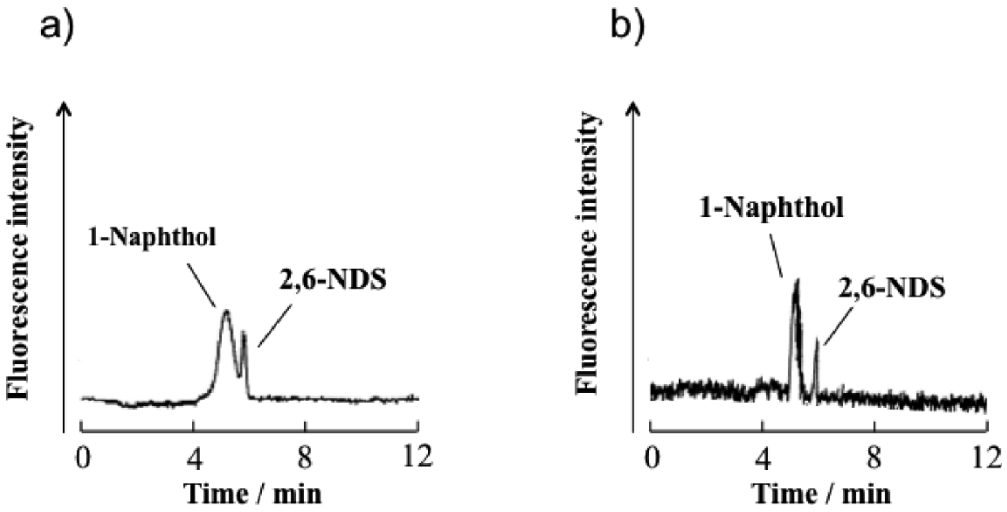

Fig. 5 Chromatograms of the present capillary TRDC system: a) 2 wt% Triton X-100 and 2.4 M KCl at 34°C and b) 2 wt% Triton X-114 at 23°C. Capillary tube: inner diameter: 75 μm, total length: 150 cm, and effective length: 100 cm; flow rate: 1.0 μL min^{-1}; and analyte concentration: 1 mM.

outer flows in a tube in the previous papers[24-28] were consistent with the present experimental data. That is, the flow characteristics of two immiscible liquids with different viscosities in a tube[24-28] strongly supported the existence of a correlation between the development of TRDP and the viscosities of the two phases for the six types of mixed solvents system examined herein.

Capillary TRDC

A capillary TRDC system was tentatively developed using a fused-silica capillary tube as the separation column and an aqueous micellar solution (2 wt% Triton X-100 and 2.4 M KCl or 2 wt% Triton X-114 solution) as a carrier solution. The Triton X-114 solution is a well-known typical micelle aqueous two-phase separation system. Hydrophobic 1-naphthol and hydrophilic 2,6-naphthalenedisulfonic acid (2,6-NDS) as a model mixture was examined in the current TRDC system. The obtained chromatograms are shown in Fig. 5 as an initial result. In this study, 1-Naphthol and 2,6-NDS were separated and detected in this order; the Triton X-114 system without salt gave better resolutions. The effects of salts on separation performance in TRDC might be examined and considered in the future with the mixed solvent solutions of water-surfactant and water-ionic liquid systems including salts. The elution order was expected based on the distribution of the aqueous micellar solution that generated a surfactant-rich inner phase (hydrophobic) and a surfactant-poor outer phase (hydrophilic). The hydrophilic outer phase acted as a pseudo-stationary phase under laminar flow conditions. The two peaks were identified according to individual analyte analyses.

Conclusions

The TRDP generates a kinetic liquid-liquid interface in a microspace upon introduction of a homogeneous mixed solvent solution in a microspace under laminar flow conditions. The factors determining the formation of the inner and outer phases in the microspace were assessed by examining the phase diagrams incorporating solubility curves, viscosities of the upper and lower phases in a batch vessel, volume ratios of the phases, and development of the TRDP using microscopy imaging. When the difference in the viscosities between the two phases was large (> approximately 0.73 mPa·s), the phase with the higher viscosity formed as the inner phase regardless of the volume ratios, whereas when the difference in viscosities was small (< approximately 0.42 mPa·s), the phase with the larger volume ratio formed as the inner phase. This finding is a gateway to future work in the TRDP research area.

Acknowledgements

This work was supported by a Grant-in-Aid for Scientific Research (C) from the Ministry of Education, Culture, Sports, Science and Technology, Japan. This work was also supported by the Advanced Study for Integrated Particle Science and Technology, Strategic Development of Research Infrastructure for Private Universities, the Ministry of Education, Culture, Sports, Science and Technology, Japan.

References

1. K. E. Gutowski, G. A. Broker, H. D. Willauer, J. G. Huddleston, R. P. Swatloski, J. D. Holbrey, and R. D. Rogers, *J. Am. Chem. Soc.*, **2003**, *125*, 6632.
2. Z. Li, Y. Pei, H. Wang, J. Fan, and J. Wang, *TrAC, Trends Anal. Chem.*, **2010**, *29*, 1336.
3. Y. Lu, W. Lu, W. Wang, Q. Guo, and Y. Yang, *Talanta*, **2011**, *85*, 1621.
4. C. Wua, J. Wanga, H. Wanga, Y. Pei, and Z. Li, *J. Chromatogr. A*, **2011**, *1218*, 8587.
5. J. Han, Y. Wang, Y. Li, C. Yu, and Y. Yan, *J. Chem. Eng. Data*, **2011**, *56*, 3679.
6. H. Watanabe and H. Tanaka, *Talanta*, **1978**, *25*, 585.
7. K. Fujinaga, *Anal. Sci.*, **1993**, *9*, 479.
8. T. Saitoh, H. Tani, T. Kamidate, and H. Watanabe, *TrAC, Trends Anal. Chem.*, **1995**, *14*, 213.
9. T. M. Z. Moattar and R. Sadeghi, *Fluid Phase Equilib.*, **2002**, *203*, 177.
10. P. L. Trindade, M. M. Diogo, D. M. F. Prazeres, and C. J.

Marcos, *J. Chromatogr. A*, **2005**, *1082*, 176.
11. T. I. Horváth and J. Rábai, *Science*, **1994**, *266*, 72.
12. K. Nakashima, F. Kubota, M. Goto, and T. Maruyama, *Anal. Sci.*, **2009**, *25*, 77.
13. J. Lim and T. M. Swager, *Angew. Chem., Int. Ed.*, **2010**, *49*, 7486.
14. H. Matsuda, A. Kitabatake, M. Kosuge, K. Tochigi, and K. Ochi, *Fluid Phase Equilib.*, **2010**, *297*, 187.
15. C. Dennis and Z. R. Lee, *Green Chem.*, **2001**, G3.
16. M. Masato, M. Hasegawa, D. Sadachika, S. Okamoto, M. Tomioka, Y. Ikeya, A. Masuhara, and Y. Mori, *Tetrahedron Lett.*, **2007**, *48*, 4147.
17. T. Maruyama, K. Nakashima, F. Kubota, and M. Goto, *Anal. Sci.*, **2007**, *23*, 763.
18. N. Jinno, M. Murakami, K. Mizohata, M. Hashimoto, and K. Tsukagoshi, *Analyst*, **2011**, *135*, 927.
19. M. Murakami, N. Jinno, M. Hashimoto, and K. Tsukagoshi, *Anal. Sci.*, **2011**, *27*, 793.
20. S. Fujinaga, K. Unesaki, S. Negi, M. Hashimoto, and K. Tsukagoshi, *Anal. Methods*, **2012**, *4*, 3884.
21. K. Tsukagoshi, *Anal. Sci.*, **2014**, *30*, 65.
22. Y. Kudo, H. Kan, N. Jinno, M. Hashimoto, and K. Tsukagoshi, *Anal. Methods*, **2012**, *4*, 906.
23. Y. Masuhara, N. Jinno, M. Hashimoto, and K. Tsukagoshi, *Anal. Sci.*, **2012**, *28*, 439.
24. A. E. Everagae, *Trans. Soc. Rheol.*, **1973**, *17*, 629.
25. H. Sotjthernj and N. L. Ballmar, *Appl. Polym. Symp.*, **1973**, *20*, 175.
26. J. L. White and B. L. Lee, *Trans. Soc. Rheol.*, **1975**, *19*, 457.
27. D. L. Maclean, *Trans. Soc. Rheol.*, **1973**, *17*, 385.
28. D. D. Joseph, Y. Renardy, and M. Renardy, *J. Fluid Mech.*, **1984**, *141*, 309.